Twenty-Sixth Symposium (International) on Combustion/The Combustion Institute, 1996/pp. 1395–1403

CHEMICAL EFFECTS OF CF_3H IN EXTINGUISHING COUNTERFLOW CO/AIR/H_2 DIFFUSION FLAMES

G. S. FALLON AND H. K. CHELLIAH
Department of Mechanical, Aerospace, and Nuclear Engineering
University of Virginia
Charlottesville, VA 22903, USA

G. T. LINTERIS
Building and Fire Research Laboratory
National Institute of Standards and Technology
Gaithersburg, MD 20899, USA

The relative importance of introducing CF_3H as a fire suppressant with the oxidizer or the fuel stream, and its chemical and thermal effects on the extinction condition of counterflow CO/air/H_2 *diffusion* flames, are investigated both experimentally and numerically. In experiments, the extinction strain rate is evaluated by measuring the jet exit velocities at extinction and the jet separation distance. In numerical calculations, the potential flow approximation is introduced to describe the outer flow field and the strain rate at extinction is determined from the axial velocity gradient on the oxidizer side. By employing mixture fraction concepts, the shift in flame location within the mixing layer caused by increasing the CF_3H mole fraction or switching CF_3H from air to fuel stream is shown to affect the measured and predicted extinction strain rates significantly. Flame structure and reaction pathway analyses have been used to identify the rate-controlling reactions and the influence of introducing the suppressing agent from the oxidizer or fuel side on the finite-rate chemistry. Subsequent sensitivity analysis has shown that two alternate CF_3-consumption reaction pathways can either increase or decrease the extinction strain rate, similar to the sensitivities found in a recent premixed burning velocity study. Finally, based on the numerical calculations, the overall chemical and thermal effects of CF_3H are demonstrated by freezing the CF_3H chemistry and by replacing the heat capacity of CF_3H with that of N_2 for the frozen case.

Introduction

Chemical fire-suppressing agents containing Br atoms, notably bromotrifluromethane (CF_3Br—halon 1301), have been used extensively in the past to suppress fires in aircrafts, engine compartments, flammable liquid pools, electronic equipment, and so forth. As stipulated by the Montreal Protocol and subsequent amendments, the new production of halon 1301 has been banned as of January 1994 because of its high ozone depletion potential (ODP) [1,2]. Of the alternate zero ODP chemical suppressants considered, fluorinated hydrocarbons have attracted considerable attention [2,3]. Most of the modeling efforts aimed at understanding the flame-suppression mechanism of these compounds have been based on premixed systems in which the fluorinated agent is well mixed with fuel and oxidizer [4–7]. The motivation for such studies is understandable since the burning velocity provides a clear physicochemical parameter characterizing the effectiveness of the suppressing agent. However, most practical flames operate in non-premixed mode, and the method of introducing the inhibiting agent can play an important role in determining the extinction characteristics. By employing a counterflow CO/air/H_2 diffusion flame, with the agent introduced to either stream, the effectiveness of one of the simplest fluorinated hydrocarbons, namely CF_3H, is investigated here, both experimentally and numerically. In numerical calculations, a detailed chemical kinetic model involving 23 species in 60 elementary reactions has been employed and the basic chemical and thermal suppression mechanisms are analyzed. Comparisons with experimentally measured extinction conditions are also presented.

In hydrocarbon flames, CO is a dominant intermediate product of combustion and its oxidation path is often the rate-limiting step. Therefore, the basic understanding obtained on the suppression of CO/air/H_2 diffusion flames by CF_3H can be extended to other hydrocarbon/air systems, with some minor modifications of the hydrocarbon decomposition pathways because of the presence of fluorinated compounds. The use of CO as the fuel also considerably simplifies the modeling of finite-rate

chemistry effects and removes the many uncertainties associated with the reaction rate constants of fluorinated intermediate species (e.g., CF_3) with hydrocarbons and their intermediates. Although the alternate chemical suppressants considered to date are dominated by two- and three-carbon fluorinated molecules [2], the simpler CF_3H (which is being used currently in several European countries) can provide important information about, for example, the inhibition mechanism by the CF_3 intermediate. The radical scavenging by CF_3 also contributes to the inhibition mechanism of CF_3Br and has been investigated previously [8]. However, because of the dominant suppression by brominated species, no clear effort has been made to characterize the inhibition potential of such fluorinated species, especially on non-premixed flames.

Counterflow CO/H_2/air diffusion flames have been used previously to analyze the interaction between finite-rate chemistry and flow field effects, both experimentally [9] and theoretically [9–11], by changing the jet exit velocities and measuring the flame response to the changing flow residence time. The goal of the present study is to employ a similar flow configuration to test the validity of recently proposed chemical kinetic models for CF_3H [5,12] and obtain an understanding of the chemical and thermal effects of such fire-suppressing agents. The extraction of such fundamental information requires careful consideration of the flame location in the mixing layer and accurate description of the local flow residence time. Using a Lewis number of unity for the major reactants, the mixture fraction concepts are employed here to simplify the analyses of the flame structure and its extinction conditions. Four broad cases are considered (i.e., depending on whether CF_3H and H_2 are introduced with the air or fuel stream), but only some selected results are presented here for brevity. Variations in the location of the H_2 and CF_3H addition allow control over the flux of F and H to the reaction zone and the species with which they can react, greatly affecting the kinetics.

Experimental Procedure

The counterflow diffusion flame experiments were conducted at the National Institute of Standards and Technology (NIST). The burner consists of two jets of 2.22-cm inner diameter separated by 1.1 cm [13], each jet containing a number of fine-wire screens (60 mesh/cm) to provide a uniform flow. The upper jet, used for the fuel stream, is surrounded by a water-cooled heat exchanger. Mild suction draws the combustion products through the heat exchanger and into the exhaust. The lower jet is surrounded by an annulus, where co-flowing nitrogen gas shields the flame from room air; this additional nitrogen also reduces the tendency for afterburning of any unreacted fuel and air in the exhaust system. The burner is located in a chemical fume hood because of the toxicity of HF and CF_2O.

The flows of air, CO (Matheson, 99.9%), H_2 (Matheson, 99.9995%), and CF_3H (Dupont) are regulated with digitally controlled mass flow controllers (Sierra Model 860) with a claimed precision of 0.2% and accuracy of 1% of full scale and are calibrated with bubble and dry (American Meter Co. DTM-200A) flow meters so that their accuracy is ±2%. (Certain trade names and company products are mentioned in the text or identified in illustrations to specify adequately the experimental procedure and equipment used. In no case does such identification imply recommendation or endorsement by the NIST, nor does it imply that the products are necessarily the best available for the purpose.) House compressed air (filtered and dried) is used after it is additionally cleaned by passing it through a 0.01 μm filter, a carbon filter, and a desiccant bed to remove small aerosols, organic vapors, and water vapor.

The strain rate, seen as the maximum value of the oxidizer-side axial velocity gradient, just before the mixing layer, is approximated from the outer flow jet exit velocities according to Ref 14:

$$k = (2|v_0|/L)[1 + |v_F|\sqrt{\rho_F}/(|v_0|\sqrt{\rho_0})] \qquad (1)$$

Here, L denotes the distance between the ducts, v the velocity, ρ the density, and the subscripts F and 0 the fuel and oxidizer stream. The jet exit velocities are chosen so that the momentum of the two streams is equal; that is, $\rho_F v_F^2 = \rho_0 v_0^2$. Doing so ensures that the flame, which is usually close to the stagnation plane, is kept approximately equidistant from the two jets. Inserting the momentum balance into Eq. (1) yields $k = 4|v_0|/L$.

Computer control of the experiments allows independent specification of the strain and the inhibitor and hydrogen mole fractions in the fuel or air streams, while maintaining equal jet momenta. In operation, the values of the species mole fractions are held constant while the total flows are increased. When the critical value of the strain rate is reached, the flame extinguishes abruptly and the flow values are recorded.

Numerical Calculations

The counterflow field established between two opposed circular jets is assumed to be steady and laminar. For planar flames, the conservation equations governing mass, momentum, energy, and species can be written as ordinary differential equations along the axis of symmetry. Methods of integrating these equations numerically are now well established, and further details of the mathematical formulation, including the relevant boundary conditions, and the

TABLE 1
Elementary reactions in CF_3H submechanism

(1) $CF_3H + H = CF_3 + H_2$	(2) $CF_3H + OH = CF_3 + H_2O$	(3) $CF_3H + O = CF_3 + OH$
(4) $CF_3H + F = CF_3 + HF$	(5) $CF_3 + H = CF_2 + HF$	(6) $CF_3 + O = CF_2O + F$
(7) $CF_3 + F = CF_4$	(8) $CF_3 + O_2 = CF_3O + O$	(9) $CF_3 + OH = CF_2O + HF$
(10) $CF_3 + HO_2 = CF_3O + OH$	(11) $CF_4 + H = CF_3 + HF$	(12) $CF_3O + M = CF_2O + F$
(13) $CF_3O + H = CF_2O + HF$	(14) $CF_2 + H = CF + HF$	(15) $CF_2 + O = CFO + F$
(16) $CF + O_2 = CFO + O$	(17) $CF + H_2O = CHFO + H$	(18) $CHFO + M = CO + HF$
(19) $CHFO + H = CFO + H_2$	(20) $CHFO + O = CFO + OH$	(21) $CF_2O + H = CFO + HF$
(22) $CFO + M = CO + F$	(23) $CFO + H = CO + HF$	(24) $CFO + O = CO_2 + F$
(25) $CFO + OH = CO_2 + HF$	(26) $CFO + F = CF_2O$	(27) $CFO + CF_3 = CO + CF_4$
(28) $HF + M = H + F$	(29) $H_2 + F = H + HF$	(30) $OH + F = O + HF$
(31) $HO_2 + F = O_2 + HF$	(32) $H_2O + F = OH + HF$	

numerical integration procedure can be found elsewhere [15–18]. In the present calculations, a chemical kinetic mechanism having 23 species in 60 elementary reactions is employed. The numerical code used also includes full thermodynamic [19] and transport data [20] for the species in the system.

It has been shown previously that significant differences in absolute extinction strain rates (which is defined as the axial velocity gradient on the oxidizer side) are possible, depending on the description of the flow field outside the mixing layer established by the opposed jets [18]. However, the trends of extinction strain rates predicted were shown to be very similar irrespective of differences in the outer flow description. In the experiments reported here, only the jet exit velocities and jet separation distance are recorded and no detailed measurements of the flow field are made. Thus, the numerical results reported here are obtained with a potential flow approximation for the outer flow regions and only comparisons of trends, rather than absolute values, with the experimentally measured extinction strain rates could be drawn.

For non-premixed flames with Lewis number close to unity, a conserved quantity identified as the mixture fraction (Z) offers a convenient normalized scale with which to plot different flame structures and determine a characteristic extinction condition, that is, the scalar dissipation rate (χ) [21,22]. In the present calculations, the mixture fraction was evaluated by integrating its conservation equation. The scalar dissipation rate was then evaluated with the definition $\chi = 2D(dZ/dz)^2$, where D is the mass diffusion coefficient assumed to be equal to $\lambda/\rho c_p$. Here, z denotes the axial physical coordinate and λ and c_p are the thermal conductivity and specific heat capacity of the gas mixture, respectively. In general, χ varied across the mixing layer and its value at the stoichiometric flame location is reported here.

Chemical Kinetic Mechanism

The CO-oxidation mechanism, in the presence of H_2, has been adopted from Yetter et al. [23] and includes 12 species in 28 elementary reactions. The fluorinated chemistry reactions employed are a subset of that developed by NIST [5,12] and consist of 11 species in 32 reversible elementary reactions. A listing of reactions of this subset is given in Table 1. (The complete reaction rate data can be requested by e-mail from: harsha@virginia.edu.)

At near extinction flame conditions, for the four cases considered, that is, (a) CF_3H in CO stream and H_2 in air stream, (b) CF_3H and H_2 in CO stream, (c) CF_3H and H_2 in air stream, and (d) CF_3H in air stream and H_2 in CO stream, the percentile reaction flux rates of key fluorinated reactions are shown in Fig. 1. The mole fractions of CF_3H (X_{CF_3H}) and H_2 (X_{H_2}) used in each case are listed in Fig. 1, with subscripts $-\infty$ and ∞ identifying oxidizer and fuel streams. The CF_3H mole fractions in Fig. 1 are selected to yield an extinction strain rate of 325 s^{-1} (using Eq. [1]), with H_2 mole fraction held constant at 2.5%. As discussed in the next section, the influence of CF_3H on the stoichiometric flame location can produce differences in the stoichiometric scalar dissipation rates at extinction (χ_{st} indicated in Fig. 1). The H_2 has only a minor effect on the flame location because of the small percentage added.

For the present hydrogen-deficient case (see the next section for a definition), the CF_3H decomposition reactions with all four radical species H, OH, O, and F are seen to be important, especially for case (a), where CHF_3 is added to the CO stream and H_2 to the air stream. In contrast, for fluorine-deficient premixed systems, CF_3H reaction with F was found to be negligible [7]. Present results also show that, for case (d), CF_3H added to the air stream and H_2 to the CO stream (probably the most commonly encountered configuration during fire suppression, except with a higher H_2 loading), yields the highest flux rate for reaction (4) ($CF_3H + F \rightarrow CF_3 + HF$). This high flux rate of reaction (4) can be related directly to reaction (6) ($CF_3 + O \rightarrow CF_2O + F$), see Fig. 1, since a balance exists at this flame location between F-atom production and consumption by

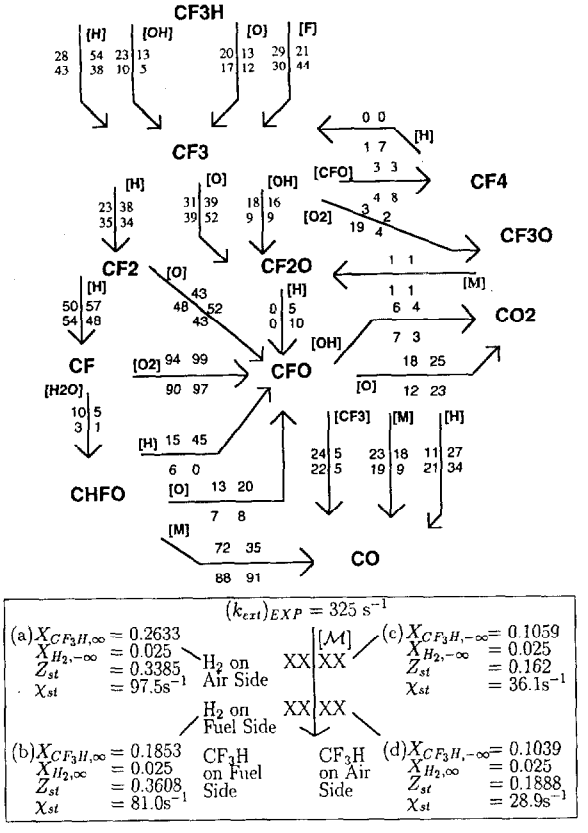

FIG. 1. Reaction pathway of fluorinated species for four different configurations of H_2 and CF_3H addition to air and fuel streams. All four cases are shown at extinction with an experimental strain rate of 325 s^{-1}. The numbers on either side of the arrows give the percentage of species consumed in reaction with the indicated species [$\mathcal{M}$].

these two reactions. The CF_3 formed by decomposition of CF_3H is subsequently oxidized to form CF_2O, which is fairly stable, or is further decomposed and oxidized to form CO, mainly through the path $CF_3 \rightarrow CF_2 \rightarrow CF \rightarrow CFO \rightarrow CO$. Implications of these alternate paths on the extinction strain rate are discussed in the next section.

Since completion of the present numerical investigation, several changes have been made to the CF_3H submechanisms [24,25]. Primarily, the CF_3H decomposition reaction with H has been modified to give a lower rate. However, as will be discussed, the most sensitive inhibition reactions are reactions (5) and (6), and, thus, these changes have minor effects on the global extinction conditions reported here.

Influence of CF_3H on Flame Location and Flame Structure

The fluorine atoms in CF_3H act as an oxidizer and can react with hydrogen to form hydrofluoric acid (HF). The thermodynamic equilibrium favors the formation of HF over water. In a hydrogen-deficient environment, the remaining F atoms lead to formation of CF_2O. Thus, the stoichiometry of the overall reaction will depend on the CF_3H and H_2 content in the reactant streams. In diffusion flames considered here (and in other hydrocarbon/air diffusion flames with halogenated fire suppressants), a shift in the stoichiometry can move the flame location within the mixing layer and have a dramatic effect on the predicted or measured extinction strain rates.

For case (d) in which CF_3H is introduced with the airstream and H_2 with the CO stream, with H_2 in deficient amount (i.e., $3\nu_{CF_3H} > \nu_{CF_3H} + 2\nu_{H_2}$), no significant formation of H_2O occurs. Thus, the overall stoichiometric reaction can be written as

$$(2 - \nu_{CF_3H} - \nu_{H_2})CO + \nu_{H_2}H_2 + (O_2 + \nu_{N_2}N_2 + \nu_{CF_3H}CF_3H) \rightarrow (2 - \nu_{CF_3H})CO_2 + (\nu_{CF_3H} + 2\nu_{H_2})\,HF + (\nu_{CF_3H} - \nu_{H_2})\,CF_2O + \nu_{N_2}N_2 \quad (2)$$

For case (d), with species mass fractions in the oxidizer stream $Y_{O_2,-\infty} = 0.18$, $Y_{CF_3H,-\infty} = 0.22$, $Y_{N_2,-\infty} = 0.60$ and fuel stream $Y_{CO,\infty} = 0.9982$, $Y_{H_2,\infty} = 0.0018$, and with $T_{-\infty} = T_{\infty} = 300$ K, Figs.

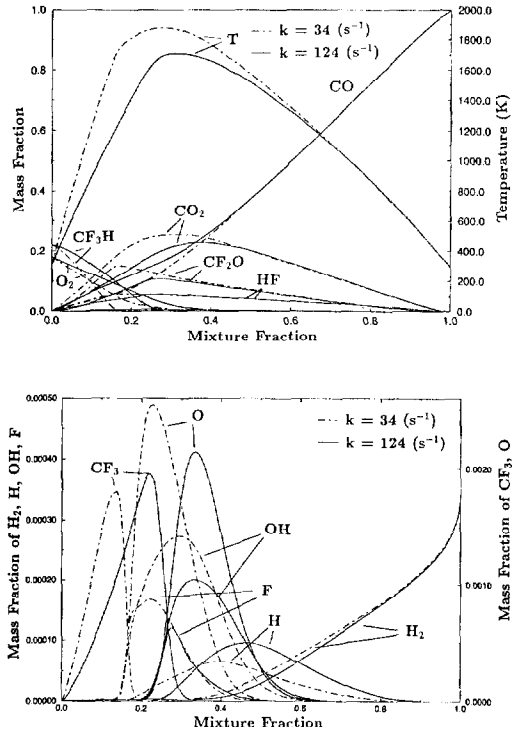

FIG. 2. (a) Major species mass fractions and temperature versus mixture fraction for the case CF_3H added to the air side and H_2 added to the fuel side for two strain rates, k = 34 s^{-1} and k = 124 s^{-1} (near extinction). (b) Minor species profiles for same conditions as in Fig. 2(a).

2a (major species and temperature) and 2b (minor species) show a comparison of the flame structure predicted for low (dashed lines) and high (solid lines) strain rates, plotted against the mixture fraction scale Z. For these mass fractions, with ν_{N_2} = 3.76 for air, the unknown stoichiometric coefficients in Eq. (2) are ν_{CF_3H} = 0.588, ν_{H_2} = 0.037. Using the expression [22]

$$Z_{st} = \left[1 + \frac{Y_{CO,\infty}/(\nu_{CO}W_{CO})}{Y_{O_2,-\infty}/(\nu_{O_2}W_{O_2})}\right]^{-1} \qquad (3)$$

with $\nu_{CO} = (2 - \nu_{CF_3H} - \nu_{H_2})$, ν_{O_2} = 1 and the molecular weight of species i identified as W_i, the stoichiometric mixture fraction Z_{st} = 0.185 is obtained. If the chemical reactions involving CF_3H and H_2 are neglected and treated as diluents, then Z_{st} is 0.241 for the overall reaction $2CO + O_2 \rightarrow 2CO_2$.

In recent non-premixed hydrocarbon flame structure studies with halogenated fire suppressants [26–28], two separate thin fuel consumption and suppressant consumption regions were identified when the suppressing agent was added to the air stream. In the present CO/air non-premixed flames, however, the CO consumption occurs over a *wide* range in mixture fraction scale ($\Delta Z \sim 0.5$ compared to $\Delta Z \sim 0.05$ for methane/air flames), as seen in Fig. 2b by the broad OH profile, and is consistent with previous theoretical studies [9,10]. In contrast, Figs. 2a and 2b indicate that CF_3H is consumed in a relatively narrow region leading to the formation of intermediate CF_3. Figure 2a also shows a significant shift in the location of the maximum temperature with changing strain rate. Moreover, Fig. 2a indicates that at the low strain rate shown, CF_3H is consumed near Z_{st} = 0.185, corresponding to the stoichiometry given by Eq. (2), while at the high strain rate shown, CF_3H consumption occurs closer to Z_{st} = 0.241. This shift in CF_3H consumption layer with strain rate is indicated clearly by the shift in CF_3 profile shown in Fig. 2b. The insensitivity of peak CF_3 mass fraction to strain rate seen in Fig. 2b suggests that CF_3 production rate is sufficiently fast and is unaffected by the reduced flow residence time but sensitive only to the local temperature. This implies that flame temperature observed in Fig. 2a at high strain rates is controlled mainly by the incomplete consumption of CO; at low strain rates or near equilibrium conditions, both CO and CF_3H consumption affect the flame temperature and play a role in determining the flame location.

The radical H, OH, and O production regions in the present diffusion flames are determined by the competition between the production/termination reactions on either side of the reaction zone, which consequently control flame extinction. For CO flames without inhibitor, or with inhibitor added to air side, the radical depletion on fuel side is generally determined by the cross-over point of forward reaction rates of $H + O_2 = OH + O$ and $CO + H + M = HCO + M$. For uninhibited moist CO/air flames, the radical depletion on the air side is determined by the cross-over point of forward reaction rates of $H + O_2 = OH + O$ and $H + O_2 + M = HO_2 + M$. However, when the inhibitor is added to the airstream, as in Fig. 2, the main radical depletion occurs not through forward reaction $H + O_2 + M = HO_2 + M$ but because of reactions with CF_3H and CF_3. Based on numerical calculations, the variation of these forward reaction rates across the mixing layer obtained is shown in Fig. 3. The implication of these results on the flame extinction conditions is discussed next.

Because of the nonunity Lewis numbers, especially that of H_2, there can be some differences in the structure plots between the mixture fraction scale and the physical scale, for example the nonlinear profile for H_2 in the frozen region of the mixing layer in Fig. 2b; however, the main features of the flame structure are unaffected.

Flame Extinction Results

Figure 4 shows a comparison between the experimentally measured extinction strain rates and two

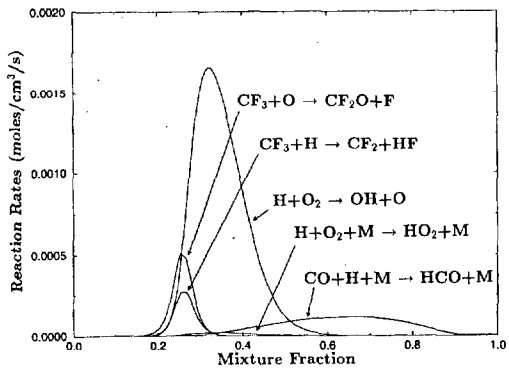

FIG. 3. Reaction flux rates versus mixture fraction for the radical production and consumption reactions for the high strain rate case shown in Fig. 2(a).

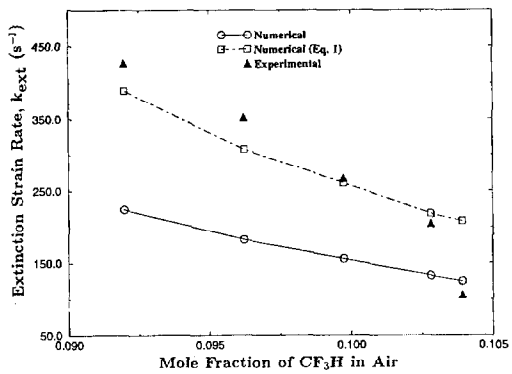

FIG. 4. Comparison of the experimental and numerical extinction strain rate versus inhibitor mole fraction with CF_3H added to the air stream and H_2 added to the fuel stream (numerical strain rate results shown as a solid line are from the axial velocity gradient and the dashed line is from Eq. [1]).

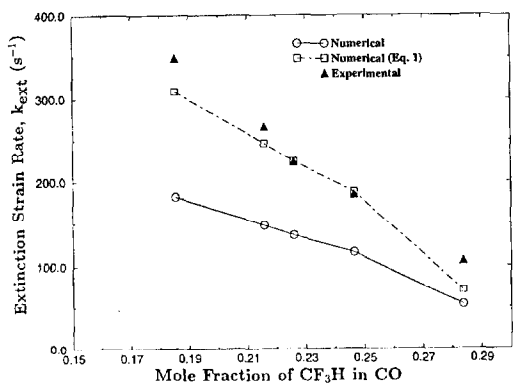

FIG. 5. Same as Fig. 4, except that CF_3H is added to the fuel stream.

sets of numerical results as a function of the CF_3H mole fraction added to the air stream. The H_2 mole fraction in the CO stream is held fixed at 0.025. The numerical results shown as the solid line are for the strain rate defined by the axial velocity gradient on the oxidizer side (assuming potential flow field), while the dashed line shown corresponds to that obtained from Eq. (1) with numerical jet exit velocities. Previous studies have shown that when the formula given by Eq. (1) is used with potential flow numerical results, the extinction strain rate is typically higher than the experimental values because of the rotational flow in experiments [18]. At lower CF_3H mole fractions in Fig. 4, however, experimental results are in fact greater than the numerical extinction results obtained using the formula, indicating a possible deficiency of the mechanism used. The general trend on adding inhibitor to the air side is predicted reasonably well.

The addition of inhibitor to the air side with hydrogen in the CO stream, case (d), is perhaps the most important practical configuration, but other configurations have been investigated to understand the chemical implications. For example, the influence of introducing CF_3H with the fuel and air stream has been investigated recently by Trees et al. [27] for a methane/air diffusion flame. With the extinction strain rate held fixed, it was shown that the amount of CF_3H needed to extinguish the flame is significantly higher when it is added to the fuel stream as compared to the air stream [27]. Similar results are obtained here when CF_3H is added to the CO stream and are shown in Fig. 5. A comparison of Figs. 4 and 5 indicates that, for an extinction strain of about 300 s^{-1}, the mole fraction of CF_3H needed in the CO stream is about twice that in the air stream.

The preceding comparison between Figs. 4 and 5, however, can be misleading because the stoichiometric flame location in the two cases is quite different. As shown in the legend of Fig. 1, for a fixed strain rate and different inhibitor loading, the stoichiometric extinction scalar dissipation rate (χ_{st}) is significantly different, although the measured extinction strain is the same. Since the local diffusion time is inversely related to the scalar dissipation rate [29], local flow residence times for the four cases are different, even if the imposed strain rate is the same. One major drawback of the present CO/air flames is that the relatively large Z_{st} introduces limitations on analytically relating the stoichiometric scalar dissipation to the strain rate, evaluated based on the outer flow field [30,31]. Irrespective of the physical differences caused by the flame location, switching of the agent from air side to fuel side affects the radical termination reactions, as shown in Fig. 3. To factor out the flame location and finite-rate chemistry effects, further analysis is needed with new experiments.

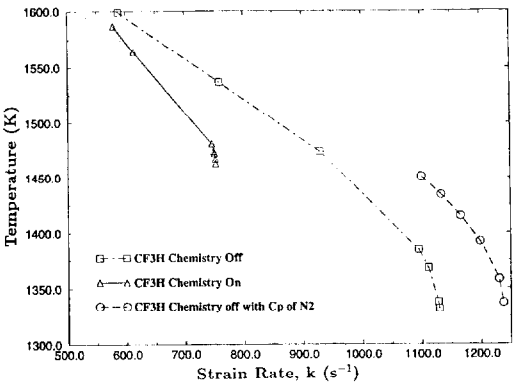

FIG. 6. The variation of peak flame temperature as a function of strain rate from numerics for the case CF_3H added to the air stream ($Y_{CF_3H,-\infty} = 0.1048$) and H_2 added to the fuel stream ($Y_{H_2,\infty} = 0.0018$). The solid line ("on") is with full elementary mechanism, the chain line ("off") is with setting CF_3H rates to zero, and the long dashed line is with frozen chemistry and c_p of CF_3H replaced by that of N_2.

In a recent *premixed* flame study [7], involving CO/air/H_2/CF_3H, the most sensitive reactions controlling the burning velocity were in fact found to be reactions (5) ($CF_3 + H \rightarrow CF_2 + HF$) and (6) ($CF_3 + O \rightarrow CF_2 + F$). In addition, sensitivity analysis has shown that an increase in reaction (6) raises the burning velocity, whereas an increase in reaction (5) decreases the burning velocity [7]. As seen in Fig. 3, reactions (5) and (6) have a major role in consuming radicals on the air side of the present CO/air/H_2 diffusion flames. Sensitivity analysis of present non-premixed flames has shown that increase in rate of reaction (5) by 5% decreases the extinction strain rate from 376 to 369 s^{-1} while 5% increase in reaction (6) increases the extinction strain rate from 376 to 379 s^{-1}, consistent with the premixed burning rate sensitivity results. Reactions (5) and (6) are exothermic, with the heat release of reaction (6) about twice that of reaction (5), and may explain partially the different sensitivities seen. However, reaction (5) traps radicals in a long CF_3 consumption chain, and its increase leads to a radical depletion and, hence, the observed decrease in extinction strain rate.

Based on the present numerical predictions, it is relatively easy to demonstrate the chemical and thermal effect of CF_3H on CO/air/H_2 diffusion flames. For example, Fig. 6 shows a comparison of the maximum flame temperature as a function of the imposed potential flow strain rate, with CF_3H chemistry turned on (triangles) and off (squares), indicating a significant chemical effect. By keeping the CF_3H in the air stream, neither thermal nor transport effects are modified. Furthermore, the magnitude of thermal effect on the predicted extinction strain rate is illustrated in Fig. 6, where the heat capacity of the nonreacting CF_3H is replaced with that of N_2. These results clearly indicate that the chemical effects of CF_3H are far more significant than the thermal effects of adding CF_3H as a high heat-capacity inert agent to the air stream.

Summary and Concluding Remarks

An experimental and numerical study was performed to evaluate the effectiveness and suppression mechanism of CF_3H in extinguishing CO/air/H_2 diffusion flames. The flame extinction condition was characterized by the flow strain rate, and the general trends predicted were shown to be in reasonable agreement with experiments.

Based on numerical calculations with a detailed chemical kinetic model, and by turning the CF_3H chemistry on and off, the chemical effect was clearly demonstrated. Flame structure and reaction pathway analyses have shown that addition of CF_3H to the air side lowers the extinction strain significantly, consistent with previous studies with other fuel/air/agent systems. This was attributed to two effects, (a) shifting of the flame location within the mixing layer and (b) the chemical effects due to radical consumption by fluorinated species on the air side, rather than the termination reaction $H + O_2 + M \rightarrow HO_2 + M$ for the uninhibited case. Sensitivity analysis has shown that an increase in reaction $CF_3 + O \rightarrow CF_2O + F$ tends to increase the extinction strain, whereas an increase in reaction $CF_3 + H \rightarrow CF_2 + HF$ tends to decrease it. However, further careful studies are needed to separate the two effects caused by flame location and finite-rate chemistry for non-premixed flames considered here and for other fuel/agent combinations. In future work, for absolute comparison of predictions with experiments, detailed measurements of the flow field, as well as rotational flow field description in the numerical calculations, must be employed.

Acknowledgments

The helpful contributions by D. Trees to the experiments are gratefully acknowledged. The authors also would like to thank Drs. D. Burgess, W. Tsang, P. Westmoreland, and M. Zachariah for helpful discussions on their mechanism. The work at NIST was supported by the U.S. Naval Air Systems Command; U.S. Army Aviation and Troop Command; Federal Aviation Administration Technical Center; and the U.S. Air Force.

REFERENCES

1. Pitts, W. M., Nyden, M. R., Gann, R. G., Mallard, W. G., and Tsang, W., "Construction of an Exploratory

List of Chemicals to Initiate the Search for Halon Alternatives," National Institute of Standards and Technology, Gaithersburg, MD, NIST TN-1279, 1990.
2. Grosshandler, W. L., Gann, R. G., and Pitts, W. M., "Evaluation of Alternate In-Flight Fire Suppressants for Full-Scale Testing in Aircraft Engine Nacelles and Dry Bays," National Institute of Standards and Technology, Gaithersburg, MD, NIST SP-861, 1994.
3. Miziolek, A. W. and Tsang, W., Eds., *Halon Replacements: Technology and Science*, American Chemical Society, Washington, D.C., 1995.
4. Vandooren, J. F., da Cruz, N., and Van Tiggelen, P., *Twenty-Second Symposium (International) on Combustion*, The Combustion Institute, Pittsburgh, 1988, p. 1587.
5. Westmoreland, P. R., Burgess, D. R. F. Jr., Zachariah, M. R., and Tsang, W., *Twenty-Fifth Symposium (International) on Combustion*, The Combustion Institute, Pittsburgh, 1994, pp. 1505–1511.
6. Bozzelli, J. W., Tsan, H. L., Anderson, W. R., and Sausa, R. C., Eastern States Section Meeting, The Combustion Institute, Clearwater, FL, December 1994.
7. Linteris, G. T., "Numerically Predicted Flame Structure and Burning Rates of Premixed CO-Ar-O_2-H_2 Flames Inhibited by CF_3H," to appear in *Combust. Flame*.
8. Westbrook, C. K., *Combust. Sci. Technol.* 34:201–225 (1983).
9. Drake, M. C. and Blint, R. J., *Combust. Flame* 76:151–167 (1989).
10. Chung, S. H. and Williams, F. A., *Combust. Flame* 82:389–410 (1990).
11. Chen, J. Y., Liu, Y., and Rogg, B., in *Reduced Kinetic Mechanisms for Applications in Combustion Systems* Vol. 15 (Peters, N. and Rogg, B., Eds.), Springer Verlag, 1993, pp. 196–223.
12. Nyden, M. R., Linteris, G. T., Burgess, D. R. F. Jr., Westmoreland, P. R., Tsang, W., and Zachariah, M. R., "Flame Inhibition Chemistry and the Search for Additional Fire Fighting Chemicals," National Institute of Standards and Technology, Gaithersburg, MD, NIST SP-861, 1994.
13. Puri, I. K. and Seshadri, K., *Combust. Flame* 65:137–150 (1986).
14. Seshadri, K. and Williams, F. A., *Int. J. Heat Mass Transfer* 21:251–253 (1978).
15. Smooke, M. D., *J. Comp. Phys.* 48:72–105 (1982).
16. Miller, J. A., Kee, R. J., Smooke, M. D., and Grcar, J. F., Paper No. WSS/CI 84-10, Western States Section, The Combustion Institute, April 1984.
17. Smooke, M. D., Puri, I. K., and Seshadri, K., *Twenty-First Symposium (International) on Combustion*, The Combustion Institute, Pittsburgh, 1986, pp. 1783–1792.
18. Chelliah, H. K., Law, C. K., Ueda, T., Smooke, M. D., and Williams, F. A., *Twenty-Third Symposium (International) on Combustion*, The Combustion Institute, Pittsburgh, 1991, pp. 503–511.
19. Kee, R. J., Miller, J. A., and Jefferson, T. H., "Chemkin: A General Purpose, Problem-Independent, Transportable, Fortran Chemical Kinetics Code Package," Sandia Report SAND 80-8003, 1980.
20. Kee, R. J., Warnatz, J., and Miller, J. A., "A Fortran Computer Code Package for the Evaluation of Gas-Phase Viscosities, Conductivities, and Diffusion Coefficients," Sandia Report SAND 83-8209, 1983.
21. Bilger, R. W., *Combust. Sci. Technol.* 13:155–170 (1976).
22. Williams, F. A., *Combustion Theory*, 2d ed., Addison-Wesley, Menlo Park, CA, 1985.
23. Yetter, R. A., Dryer, F. L., and Rabitz, H., *Combust. Sci. Technol.* 79:97–128 (1991).
24. Burgess, D. R. F. Jr., Zachariah, M. R., Tsang, W., and Westmoreland, P. R., "Thermochemical and chemical kinetic data for fluorinated hydrocarbons," National Institute of Standards and Technology, Gaithersburg, MD, NIST TN-1412, 1995.
25. Burgess, D. R. F. Jr., Zachariah, M. R., Tsang, W., and Westmoreland, P. R., accepted for publication in *Prog. in Energy Combust. Sci.*
26. Hamins, A., Trees, D., Seshadri, K., and Chelliah, H. K., *Combust. Flame* 99:221–230 (1994).
27. Trees, D., Grudno, A. D., Ilincic, N., Weissweiler, T., and Seshadri, K., *Proceedings of the Joint Technical Meeting of The Central States/Western States/Mexican National Sections*, The Combustion Institute, San Antonio, TX, April 24–26, 1995, pp. 227–232.
28. Tanoff, M. A., Dobbins, R. R., Smooke, M. D., Burgess, D. R. F. Jr., Zachariah, M. R., Tsang, W., and Westmoreland, P. R., *Eastern States Section Meeting*, The Combustion Institute, Worcester, MA, Oct. 16–18, 1995, pp. 447–450.
29. Chelliah, H. K. and Williams, F. A., *Combust. Flame* 80:17–48 (1990).
30. Peters, N., *Combust. Sci. Technol.* 30:1–17 (1982).
31. Kim, J. S. and Williams, F. A., *SIAM J. Appl. Math.* 53(6):1551–1556 (1993).

COMMENT

Phillip R. Westmoreland, University of Massachusetts, USA. With respect to Professor van Tiggelen's question about how the constant was estimated for

$$CF_3 + OH \rightarrow CF_2O + HF \quad (1)$$

the high-pressure limit for

$$CH_3 + OH \rightarrow CH_3OH \quad (2)$$

was used (Refs. 5 and 12 of the paper). Our *ab initio* calculations showed that the energy barrier for

$$CF_3OH \rightarrow CF_2O + HF \quad (3)$$

is low relative to the entrance energy to reaction 1, unlike the analogous decomposition of CF_3OH so the rate constant of reaction 1 is that of the CF_3 + OH combination rate. Refinement of the estimate by direct measurement would certainly be desirable.